Surface transitions under confinement

2002 J. Phys.: Condens. Matter 14 2211

(http://iopscience.iop.org/0953-8984/14/9/310)

INSTITUTE OF PHYSICS PUBLISHING JOURNAL OF PHYSICS: CONDENSED MATTER

J. Phys.: Condens. Matter **14** (2002) 2211–2221 PII: S0953-8984(02)31071-3

Surface transitions under confinement

J Quintana[1] **and A Robledo**[2]

[1] Instituto de Química, Universidad Nacional Autónoma de México, México 04510 DF, Mexico
[2] Instituto de Física, Universidad Nacional Autónoma de México, Apartado Postal 20-364, México DF 01000, Mexico

Received 22 November 2001
Published 22 February 2002
Online at stacks.iop.org/JPhysCM/14/2211

Abstract

We describe the modifications undergone by phase transitions associated with a planar surface when the system is confined by the presence of a second surface parallel to the first. The inhomogeneous states are studied within the Landau density functional theory, which imparts scaling properties to the order parameter profiles. We distinguish between two situations, identical and symmetrically opposed surface fields, and provide three illustrations: (i) a liquid crystal at the nematic–isotropic transition, (ii) a racemic mixture of enantiomeric species and (iii) a ternary molecular fluid mixture close to a consolute point.

1. Introduction

The study of phase transitions in films confined between parallel plates or walls has a long history [1] and to the present day there has been a continuing interest both theoretically and experimentally in this rich subject [2]. Most descriptions of the phase behaviour of films have been made in comparison with bulk phase properties, since conceptually bulk transitions are anticipated to be gradually modified in a film, phase boundaries and critical points being shifted, as its finite thickness L is made progressively smaller. The prototypical example of this continuous change is 'capillary condensation', descriptions of which date back to Lord Kelvin [3], that is, when capillary walls interact strongly with the fluid molecules, condensation of a gas into a liquid takes place at a pressure p_L smaller than the bulk phase coexistence pressure p_∞. In agreement with finite size scaling arguments there is a convergence of the coexistence curve and its associated critical point $T_c^{(L)}$ to the bulk coexistence curve with critical temperature $T_c^{(\infty)}$, of the form $T_c^{(L)} - T_c^{(\infty)} \sim L^{-1/\nu}$ when $L \to \infty$, where ν is the bulk correlation length exponent [4]. Of course, other factors intervene in changing bulk phase properties such as the interactions with the walls and the effective couplings near them. Accordingly, the combined effects of these with the finite film thickness have been incorporated in finite-size scaling theories of confined systems [1, 5].

0953-8984/02/092211+11$30.00

Parallel to this, the single effect of surface fields and coupling enhancements on phase behaviour, as described by the surface transitions and critical phenomena occurring in one-wall semi-infinite systems, has been similarly developed [6, 7]. A global phase diagram for the *wetting*, *prewetting*, *pure surface* and other transitions is known in detail from analysis based on the Landau phenomenological theory [8], and has been generally substantiated via numerical simulation studies [9]. For a simple system in magnetic language, the relevant thermodynamic field variables are: t the temperature difference to $T_c^{(\infty)}$, h the bulk field, h_1 the surface field, and g the enhancement of interactions at the surface. When h and h_1 vanish the so-called *ordinary*, *special* and *extraordinary* transitions take place at $t = 0$ when $g < 0$, $g = 0$ and $g > 0$ respectively. The *pure surface* transition also occurs when $h = h_1 = 0$ but at $t > 0$. The lines of wetting transitions ($t < 0$, $h = 0$) as well as the line of prewetting critical points ($h \neq 0$) require that the wall favours one phase, i.e. a non-vanishing surface field h_1. For $g > 0$ the pure surface transition appears as a particular point on the line of prewetting transitions (see [8, 10] for the original analysis).

Various aspects of the modification of the surface phase diagram for thin films have been known since its inception [1,11], but here we find it of interest to present some seldom discussed effects of finite size on surface transitions for two reasons. First, because this provides the opportunity to describe film phase behaviour in comparison with the properties of the one-wall semi-infinite problem as opposed to those of the bulk system. And secondly, because the phase properties obtained from the Landau theory apply not only to simple magnets and fluids but also to a variety of different systems, such as liquid crystals and complex fluid mixtures.

We have two distinct film configurations for a system with two-phase bulk coexistence: (1) identical or alike walls, when the interaction between the film medium and the walls favours the same phase. And, (2) opposing walls, when one wall favours one phase but the other the second phase. In the first case one observes 'capillary condensation' as described above. In the second case a more surprising effect takes place [12–17], for any wall separation L phase coexistence occurs only at temperatures $T < T_c^{(L)}$ located below and near the wetting transition temperature T_w of the semi-infinite one-wall system. There is now a convergence of $T_c^{(L)}$ to T_w as $L \to \infty$ [4, 12–17], and, remarkably, a single phase with long-range correlations in the directions parallel to the walls is found for the entire range $T_c^{(L)} < T < T_c^{(\infty)}$, with $T_c^{(L)} < T_w$. Since T_w is generally located far away from the bulk $T_c^{(\infty)}$ the consequences of confinement are conspicuous. The appearance of the single-phase states at $T_c^{(L)}$ can be identified as a shifted wetting transition [14], and this can be either continuous or of first order [14]. Thus, according to the choice of type of wall field, the phase behaviour of the film resembles either that of the bulk or that of the one-wall semi-infinite system, and this indicates the underlying connection between the properties of the confined system and those of the related infinite-size systems. So, the wetting phenomena associated with the one-wall system are clearly discernible in the behaviour of systems confined by opposing walls, but not so clearly in those confined by similar or identical walls.

In the following section we briefly recall the Landau density functional theory for one-dimensional inhomogeneities [18] together with some of the main features of the global phase diagram predicted by this theory for a one-wall semi-infinite system. In subsequent sections we describe modifications of the surface phase diagram when the system becomes confined and acquires slab geometry. In section 3 we consider the effect of finite size on the wetting transition. We illustrate this issue for a model liquid crystal confined by walls that compete in molecular alignment and examine the consequences for the bulk isotropic–nematic (IN) transition. We employ Landau–de Gennes free energy with symmetrically opposing wall fields that favour random parallel and homeotropic orientations, respectively, at each wall [19]. In section 4 we consider the finite size effect on the pure surface transition and on its associated

surface states. We analyse this question for a model symmetric fluid mixture confined by parallel planar walls and describe the concentration profiles and phase properties for cases of identical and symmetrically opposed fields at the walls. We focus on the occurrence of phase separation otherwise absent in bulk mixtures and find that this can take place when chemical potentials and molecular interactions are modified at the surfaces [23]. The phenomenon may find application in the resolution of racemic mixtures of enantiomers. In section 5 we consider the finite size effects on interfacial states close to the *special* transition. We describe this problem in terms of a model ternary mixture of bifunctional molecules [24] near a consolute point. The mixture model originally defined on a lattice has been used to represent some aspects of water–oil–amphiphile solutions [25, 26]. Bearing in mind the properties of bifunctional molecules, the confining walls can be modelled via a permanent molecular coat of these molecules, with the result that the surface fields and interaction enhancements can be simply adjusted via the coat composition. As an example, we describe a family of interfacial-like film concentration profiles. Section 6 contains some remarks on the scaling properties of the order parameter profiles obtained from the Landau theory.

2. Phase transitions in a slab geometry

Consider the Landau free energy functional with magnetization $m(z)$ and external field h

$$F[m] = \int_{z_1}^{z_2} \left[f_b(m) - hm + \frac{A}{2}\left(\frac{\mathrm{d}m}{\mathrm{d}x}\right)^2 \right] \mathrm{d}z + \Phi_1(z_1) + \Phi_2(z_2) \tag{1}$$

with

$$f_b(m) = atm^2 + bm^4 \tag{2}$$

where a and b are constants and $t \equiv (T - T_c)/T_c$ is the temperature distance to the critical temperature T_c. In equation (1) A is taken to be a constant and $\Phi_{1,2}$ are surface terms of the form

$$\Phi_{1,2} = -\tfrac{1}{2} g_{1,2} m_{1,2}^2 - h_{1,2} m_{1,2} \tag{3}$$

where $m_{1,2} = m(z_{1,2})$, $g_{1,2}$ are the surface coupling enhancement parameters and $h_{1,2}$ are the surface fields. For a d-dimensional system F is a free energy density in $(d-1)$-dimensional space.

The stationary solutions $\delta F = 0$ of equation (1) are obtained from

$$m' \equiv \frac{\mathrm{d}m}{\mathrm{d}z} = \pm\sqrt{\frac{2}{A}\left(f_b - hm + C_L\right)} \tag{4}$$

together with the boundary conditions

$$\pm \left.\frac{\mathrm{d}m}{\mathrm{d}z}\right|_{z_{1,2}} = -g_{1,2} m_{1,2} - h_{1,2}. \tag{5}$$

In equation (4) the prime indicates a derivative with respect to m and C_L is a constant of integration determined by the wall separation $L \equiv z_2 - z_1$, the plus and minus sign in equation (5) corresponds to the surfaces at z_1 and z_2 respectively. The thermodynamic stability of the profiles $m(z)$ obtained from the above equations can be determined by considering that the second variation of the free energy functional evaluated at $m(z)$ be positive. The types of solution that the theory predicts can be examined through the phase portraits (m, m') obtained from equation (4) for different values of t and h together with the straight-line boundary conditions given by equation (5) for different values of $g_{1,2}$ and $h_{1,2}$. Representative phase

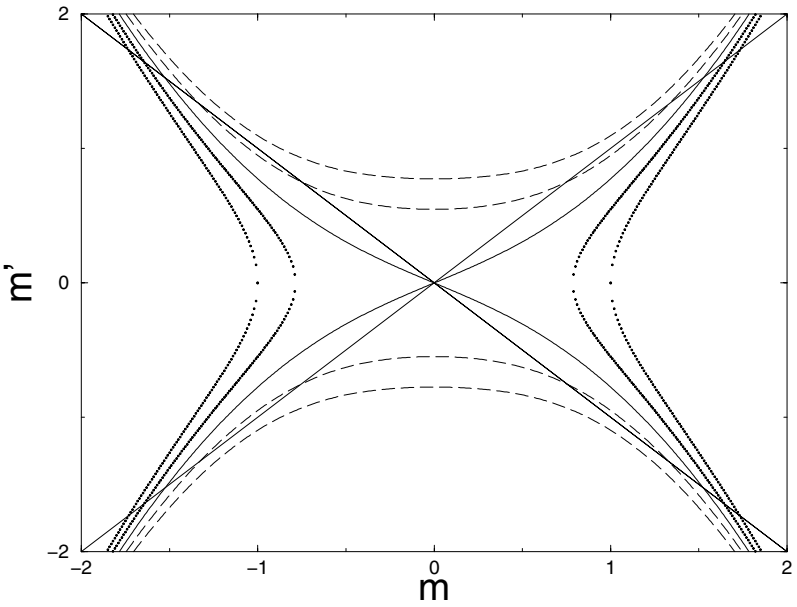

Figure 1. Phase portrait for $t > 0$ and $h = 0$. The full curve is the separatrix $C_\infty = 0$, the dashed curves are $C_L > 0$ orbits, and the dotted curves are $C_L < 0$ orbits. The straight lines represent the wall boundary conditions.

portraits are shown in figures 1–3, the conditions in figure 1 correspond to $t > 0$ and $h = 0$, those in figure 2 correspond to the bulk phase coexistence at $t < 0$ and $h = 0$, while those in figure 3 are for the same temperature $t < 0$ but $h \neq 0$, when one bulk phase is metastable. Each trajectory or orbit in these figures is obtained by assigning a value to C_L in equation (4). The possible order parameter profiles $m(z)$ for given wall fields and separations are obtained by selecting intersections of the lines with an orbit C_L that reproduces the given L. Substitution of equation (4) into (1) gives the following expression for the equilibrium (or more generally, stationary) free energy

$$F_{eq} = \int_{m_0}^{m_L} m' \,\mathrm{d}m - C_L L - \tfrac{1}{2} g_L m_L^2 - h_L m_L - \tfrac{1}{2} g_0 m_0^2 - h_0 m_0 \tag{6}$$

and differentiation of this, taking into account equation (5), gives

$$C_L = -\frac{\partial F_{eq}}{\partial L}$$

so that C_L can be associated with the force between the walls, the thermodynamic variable conjugate to L. Reference [18] provides a more detailed description of how this free energy density formalism is applied to different problems in infinite, semi-infinite and finite systems involving inhomogeneous situations, ranging from nucleation and spinodal decomposition, to wetting and surface phase transitions, and to phase diagram shifts as produced by confinement by two parallel walls.

The surface phase transitions occurring in one-wall semi-infinite systems can be seen in figures 1 to 3. The pure surface transition occurs when $t > 0$, $h = 0$, $h_1 = 0$ and $g = \sqrt{2A^{-1}at} > 0$, the relevant phase portrait orbit is the separatrix $C_\infty = 0$ in figure 1 which has a cusp at the bulk state $m = m' = 0$ at the origin. The wall boundary condition is a straight line with slope g that also passes through the origin $m = m' = 0$. This is the

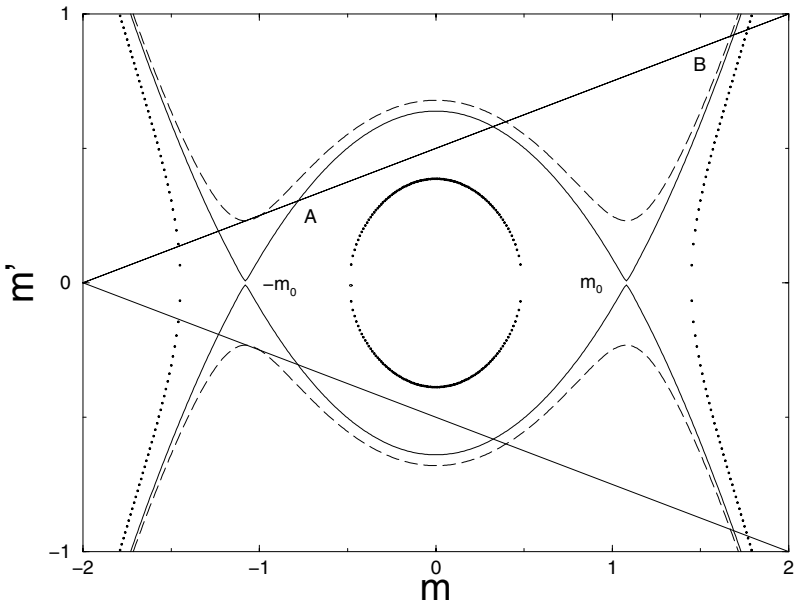

Figure 2. Phase portrait for $t < 0$ and $h = 0$. The full curve is the separatrix C_∞, the dashed curves are $C_L > 0$ orbits, and the dotted curves are $C_L < 0$ orbits. The straight line represent a wall boundary condition and the intersections A and B determine non-wetting and the complete wetting states when the bulk state is $-m_0$.

only intersection of line and orbit when g is small and $m(z) = 0$ for all z. When g is large an additional pair of intersections appears (one with $m > 0$ and $m' > 0$ and the other with $m < 0$ and $m' < 0$) and now $m(z)$ differs from zero close to the surface, there are two coexisting states $m(z)$ and $-m(z)$. The pure surface transition takes place when the orbit and the line become tangential at $m = 0$, where $\partial m'/\partial m = \sqrt{2A^{-1}at}$. The wetting transition occurs when $t < 0$, $h = 0$, $h_1 \neq 0$, when $g \geqslant 0$ it is a first-order transition but when $g < 0$ it is of second order for small values of $|h_1|$ and becomes of first order for larger $|h_1|$ at a tricritical point. In figure 2 two segments of the separatrix orbit containing the bulk state $\pm m_0$ correspond to the non-wetting and the complete wetting states, they are those between the bulk state $-m_0$ and the wall intersections at A and B respectively. The wetting transition between these two states can be located by adjusting the values of t or h_1. The prewetting transition occurs when $h \neq 0$, extends (only) out of a first-order wetting transition and terminates at a prewetting critical point. In figure 3 two segments of the separatrix orbit containing the bulk state $-m_0$ correspond to non-wetting and prewetting film states, they are those between the bulk state $-m_0$ and the wall intersections at A and B respectively. For fixed h the prewetting transition between these two states can be located by adjusting the values of t or h_1. For $g < 0$ the terminus of the wetting transitions at $t = 0$ is the *ordinary* transition, for $g > 0$ is it the *extraordinary* transition, and for $g = 0$ it is the *special* transition. In this last case the critical prewetting transitions also terminates at the *special* transition. See also [1,8] for details on the critical exponents and scaling laws associated with these transitions. The profiles $m(z)$ for the two-wall confined system are obtained from orbits other than the separatrix.

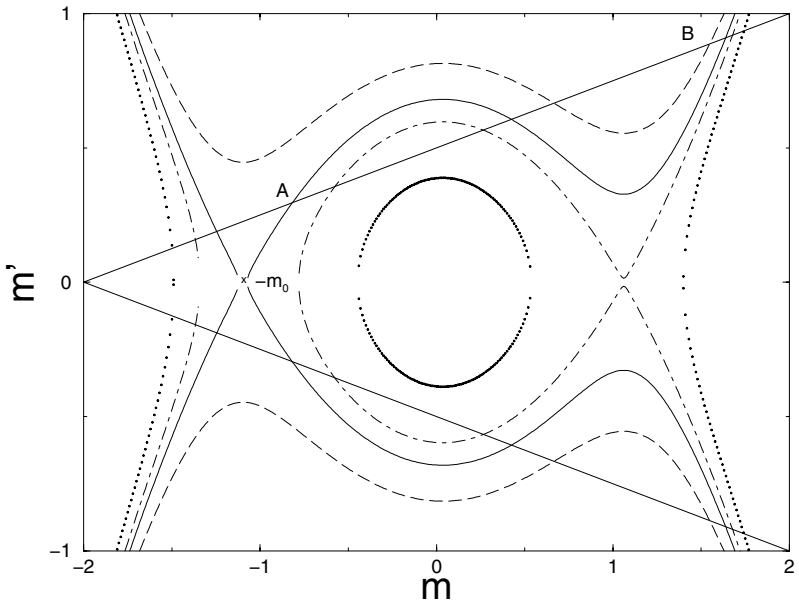

Figure 3. Phase portrait for $t < 0$ and $h < 0$. The full curve is the separatrix C_∞, the dashed curves are $C_L > 0$ orbits, and the dotted lines are $C_L < 0$ orbits. The dash-dotted orbit is another separatrix containing a uniform metastable state. The straight lines represent the wall boundaries. The straight line represents a wall boundary condition and the intersections A and B determine non-wetting and the prewetting states when the bulk state is $-m_0$.

3. Nematic liquid crystal

As an example of the effect of finite size on the wetting transition for thin films we refer to results on the alteration that the bulk IN transition suffers when confinement takes place via walls with competing surface fields [19]. We choose the surface field at one wall to favour molecular orientations parallel to the plane of the wall, with no specific preference within that plane (random parallel alignment), and that at the other wall to promote orientations normal to the plane (homeotropic alignment). Under the simplifying assumption of a uniform director orientation (normal to the walls) the Landau–de Gennes free energy [20] density functional that describes the confined liquid crystal is given by equation (1) where the magnetization m is replaced by the nematic alignment order parameter S, the magnetic field h is replaced by the ordering field μ, and where the free energy f_b is now given by

$$f_b(S) = -\mu S + a(T - T^*)S^2 + bS^3 + cS^4. \tag{7}$$

The external field strength μ is necessarily positive (since it is proportional to the square of either an electric or magnetic field applied along the z-axis). We have obtained the order parameter profiles for this arrangement with $\mu_L = -\mu_0 = \mu_s$ and $g = 0$, and we have determined the phase diagram as a function of temperature T, surface field strength μ_s and wall separation L [19].

The solutions for this problem when $T = T_{\mathrm{IN}}$ and $\mu = 0$ are equivalent to those of a magnetic slab described by a symmetric double-well Landau free energy when $h = 0$ with opposing surface fields and vanishing coupling surface enhancement g. The corresponding phase portrait is of the same type as that shown in figure 2, with m and m' replaced by S and S' respectively, and the bulk $-m_0$ and m_0 replaced by 0 and S_0 respectively. At this temperature

the one-wall semi-infinite system with isotropic bulk exhibits a wetting transition at a wall field strength $\mu_0 = \mu_s^w$, at which a wetting film of the nematic phase appears at the wall. And similarly, when the bulk state is the nematic phase a wetting transition occurs at a wall field strength $\mu_0 = -\mu_s^w$, when a wetting film of the isotropic phase develops at the wall. For the confined system with $\mu_L = -\mu_0 = \mu_s$ this transition appears shifted and occurs at a field strength $\mu_s^{qw}(L)$.

The phase properties of the liquid crystal film with symmetrically opposing walls are displayed differently when compared with the case of the magnet since the temperature in the liquid crystal with $\mu = 0$ takes the role of the external field of the magnet. This is a consequence of the cubic term in $f_b(S)$ in equation (7) that makes T the adjusting parameter for the difference in height of the minima of $f_b(S)$ and for their appearance or disappearance. Thus, NI coexistence remains fixed at $T_{\rm IN}$ under symmetrically opposing wall confinement just as spontaneous magnetization m_0 continues to takes place at vanishing h under similar circumstances. The IN transition continues to be of first order as it is the counterpart of the coexistence of oppositely magnetized states. Also, the phase behaviour observed in the nematic phase with variation of T across $T_{\rm IN}$ can be observed in the magnetic slab under the application of an external field, as h passes through zero. The competing walls introduce interfacial-like states that occupy large regions of the phase diagram where the isotropic and the nematic phase would be otherwise found.

Our study [19] indicates that the occurrence of the IN transition ($T_{\rm IN}^{(L)} = T_{\rm IN}$ for all L) is restricted to lie below a maximum wall separation $L_{qw}(\mu_s)$. The curve $L_{qw}(\mu_s)$ demarcates the transformation of 'bulk-like' IN two-phase coexistence states into 'interface-like' one-phase states. L_{qw} diverges when $\mu_s \to \mu_s^w$. The transition is of first order (L_{qw}) when μ_s is smaller than a special value μ_s^{tc} and it is critical (L''_{qw}) when μ_s is larger than μ_s^{tc}; the two branches join at a tricritical point when μ_s equals μ_s^{tc}. The IN coexistence states for $\mu_s > \mu_s^*$ undergo an additional continuous transition between low and high wall adsorption states at a locus $L'_{qw}(\mu_s)$ that originates at $L_{qw}(\mu_s^*)$ and extends towards smaller L and larger μ_s. A similar phase diagram in the (L, μ_s)-plane is obtained when the temperature is varied moderately both below and above $T_{\rm IN}$. When $T < T_{\rm IN}$ the transition at the wall separation $L_{qpw}(\mu_s)$ is between nematic- and interface-like states, whereas for $T > T_{\rm IN}$ the transition involves isotropic- and interface-like states. In both cases L_{qpw} diverges when $\mu_s \to \mu_s^{pw}$ where μ_s^{pw} is the wall field strength for a prewetting transition of the semi-infinite system at T.

4. Racemic mixture of enantiomers

As an example of the effect of finite size on the pure surface transition for thin films we consider a fluid mixture of enantiomers, i.e. molecules that are non-superimposable mirror images of each other. The pure species, termed 'right-handed' or 'left-handed', d or l, have essentially identical physical properties except when acting in chiral environments and macroscopic samples have the same phase behaviour. Generally, a mixture of the two species lacks liquid–liquid immiscibility but in some cases there is segregation in the solid phase. A mixture of equal amounts of the two species is called a racemic mixture [21].

To study phase behaviour of mixtures of enantiomers under confinement, we looked recently [23] at the properties of an elemental van der Waals symmetric mixture model [22] of equal-sized molecules with negative heat of mixing, i.e. unlike pair attractions are stronger than like pair attractions. In correspondence with the behaviour of real enantiomeric mixtures the model bulk phase diagram lacks liquid–liquid immiscibility and the racemic mixture is an azeotrope [21]. We found that phase separation of the two compounds can be induced

in the racemic mixture via confinement by means of suitable surface fields and interaction enhancements. We studied the inhomogeneous states of the racemic mixture for the slab geometry, with identical and symmetrically-opposed surface chemical potentials. The specific strength of the surface chemical potentials and the selective enhancement of interactions at the walls can be conceived to be the result of the preparation of the substrates by a uniform, oriented coating of one of the enantiomeric species or by another suitable pure enantiomer. Two different sets of identical substrates are realized with use of either the l or the d species, whereas the symmetrically opposed walls are constructed by coating one wall with the l species and the other with the d species.

The free energy of the model fluid mixture at constant density is equivalent to that of a magnetic spin-$\frac{1}{2}$ system with negative (antiferromagnetic) coupling [23]. Here again we can employ the density functional and the results for one-dimensional inhomogeneities described in section 2 [18]. In this equivalence the magnetization m measures the concentration of species $m = 1 - 2\rho_l(\rho_l + \rho_d)^{-1}$ where ρ_l and ρ_d are the number densities of the two species. The field h measures the difference $h = (\mu_d - \mu_l)/2$ between the chemical potentials μ_l and μ_d of the two species, whereas the coupling J relates to the difference $J = (\alpha - \alpha')(\rho_l + \rho_d)/2$ between the strengths α and α' of the attractive interactions for like and unlike molecular pairs. Therefore liquid–liquid immiscibility for a racemic mixture corresponds to the onset of spontaneous magnetization, and this is only possible for a ferromagnetic coupling $J > 0$. (As it is customary, the term at in $f_b(m)$ in equation (2) is given by $at = J - kT/2$, with the coordination number omitted.)

Our main results are [23]: first, there is local phase separation of the racemic mixture ($h = 0$) in the neighbourhood of the substrates for the unconfined system ($L \to \infty$) with vanishing wall fields ($h_{1,2} = 0$) but in the presence of sufficiently large surface coupling enhancement ($g > 0$). The equilibrium state is a degenerate four-phase state, i.e. four concentration profiles (two symmetric and two antisymmetric) have the same minimum free energy (see the four intersections of the straight lines with the separatrix in figure 1 that indicate the boundary conditions for these states). This state is analogous to that obtained at temperatures $T > T_c$ below the so-called purely surface transition in semi-infinite systems with ferromagnetic interactions [1]. Secondly, for the confined system ($L < \infty$) the four-phase state splits into two different two-phase states, one is the coexistence of states with profiles that show local excess concentration of the same enantiomer at both walls (symmetric profiles obtained from orbits left and right of the separatrix), and the other is the coexistence of states with profiles that show local excess concentration of a different species at each wall (antisymmetric profiles obtained from orbits above and below the separatrix). The former is the equilibrium state and the latter is metastable, and as L decreases the free energy difference between the two types of coexisting states increases. Thirdly, when the wall fields are turned on, one of these coexistence states splits into two one-phase states whereas the other remains a two-phase state. For identical walls it is the symmetric two-phase state that splits and the new equilibrium one-phase state is that rich in the enantiomer species favoured by the walls; the enrichment takes place all across the slit although it is more pronounced at the walls. For symmetrically opposing walls it is the antisymmetric two-phase state that splits, and of these, it is the state which exhibits wall enrichment in the enantiomer species favoured by the field at each wall that attains the lower free energy. For large L this is the equilibrium state. The enrichment takes place only at the walls and the mixture remains racemic at the middle of the slit. As the wall separation L decreases the free energy difference between this state and the symmetric two-phase state decreases and at a given separation there is a first-order transition below which the equilibrium configuration is that of the symmetric two-phase state.

The effect of confinement of the mixture model is a phase behaviour considerably more complex than that displayed by the bulk mixture. The coexistence of confined states rich in each of its components is the film extension of the coexisting surface states associated with the pure surface transition in the one-wall semi-infinite system. We notice that a pure surface transition of the ferromagnetic type can also take place at the surface of a system that is an antiferromagnet in bulk.

5. Three-component fluid mixture

As a third example of film phase behaviour we consider a fluid mixture that exhibits liquid–liquid immiscibility. A model ternary mixture of bifunctional molecules was designed long ago [24] to describe solubilization of two otherwise immiscible fluids and to verify whether consolute points (liquid–liquid criticality) have the same properties as ordinary liquid–gas critical points. Subsequently the model and its generalizations were employed to describe properties of solutions of amphiphiles [25,26]. The mixture consists of three species of linear bifunctional molecules, each molecule having two ends that can be of two different types, A or B. The molecules are denoted by AA , BB and AB, and are placed on the bonds of a regular lattice. In all the mixture configurations all the lattice bonds are (singly) occupied and the molecules are placed such that only ends of the same type meet at any lattice point. This construction rule makes the model mixture equivalent to an Ising spin-$\frac{1}{2}$ model with the spins placed on the sites of the same lattice where the external field h and the spin coupling J are given by

$$h = \mu_{BB} - \mu_{AA} \tag{8}$$

and

$$J = \tfrac{1}{2}(\mu_{BB} + \mu_{AA}) - \mu_{AB} \tag{9}$$

where μ_{AA}, μ_{BB} and μ_{AB} are the chemical potentials of the three species (and where some proportionality constants involving the lattice coordination number have been omitted). We notice that both ferromagnetic (low concentration of species AB) and antiferromagnetic (high concentration of AB) behaviour is displayed by the phase properties of the mixture.

We can study the inhomogeneous states of this mixture model in continuum space by considering the Landau density functional in equations (1) and (2) and by relating the bulk field h and the temperature difference t to the mixture chemical potentials via equations (8) and (9) with $at = J - kT/2$. The relationship between the magnetization $m(z)$ and the densities of the mixture $\rho_{AA}(z)$, $\rho_{BB}(z)$ and $\rho_{AB}(z)$ is given by $m(z) = \rho_{BB}(z) - \rho_{AA}(z)$. This simplest version of the model that is equivalent to a spin-$\frac{1}{2}$ system requires that $\rho_{AA}(z) + \rho_{AB}(z) + \rho_{BB}(z) = 1$. The surface fields and enhancement parameters in equations (3) can be related similarly to substrate chemical potentials acting on the mixture via

$$h_{1,2} = \mu_{BB}^{(1,2)} - \mu_{AA}^{(1,2)} \tag{10}$$

and

$$J_{1,2} = \tfrac{1}{2}\left(\mu_{BB}^{(1,2)} + \mu_{AA}^{(1,2)}\right) - \mu_{AB}^{(1,2)} \tag{11}$$

where the sub- and superscripts 1 and 2 refer to the walls that confine the film. The coupling enhancements $g_{1,2}$ are given by $g_{1,2} = (J_{1,2} - J)/J - 1$ (coordination number factors again omitted). The characteristics of the model imply a method of 'preparation' of the substrates for 'tuning in' the system to any desired location of the one-wall global phase diagram (h, t, h_1, g) or its extension for the film of finite thickness L. Each substrate is prepared with a coat of given concentration of the bifunctional molecules AA, BB and AB that fixes the values of

the surface chemical potentials $\mu_{BB}^{(1)}$, $\mu_{AA}^{(1)}$, $\mu_{AB}^{(1)}$ and $\mu_{BB}^{(2)}$, $\mu_{AA}^{(2)}$, $\mu_{AB}^{(2)}$. Thus, for example, the *special* transition in the semi-infinite system is obtained by giving the bulk mixture (at temperature T) equal amounts of the species AA and BB ($h = 0$) and adding species AB to reduce the spin coupling J until the consolute point is reached ($t = 0$). The surface is prepared with a monolayer also containing equal amounts of AA and BB ($h_1 = 0$) and the filling of the monolayer is completed by an amount of AB such that a value of J_1 is achieved at which g vanishes.

Consider the closed orbits inside the separatrix containing the uniform bulk states $\pm m_0$ in the phase portrait in figure 2. The inhomogeneous states associated with these orbits are periodic unstable stationary states of the bulk spinodal decomposition [27]. The modification of these states for the slab geometry can be described as a family of film states with interfacial-like concentration profiles in the z-direction for the mixture model when conditions are close to the *special* transition, when $h = h_1 = g = 0$ but $t < 0$. These closed orbits are split in halves by their intersections with the horizontal axis $m' = 0$, the boundary condition for the walls with $h_1 = g = 0$. Each half orbit produces one concentration profile in this family, that in the limit $L \to \infty$ becomes the interface enriched in species AB between two bulk liquids rich in species AA and BB respectively. For the confined system the film profile with decreasing L is obtained from closed orbits located progressively farther away from the separatrix and towards the centre of the portrait.

6. Scaling properties of the order parameter

The order parameter profiles $m(z)$ obtained via the minimization of equation (1) always display scaling properties as the range of validity of the Landau theory is the neighbourhood of a classical critical point. Specifically, by construction of equation (1), a scaling property should be exhibited by all profiles related to bulk, surface and confined states. Scaling of profiles is to be found for different approaches to the critical point, e.g.: the approach from below T_c at vanishing h, that for the vanishing of a (possibly non-uniform) field h at $t = 0$, or when the width of a slab L diverges at $t \lesssim 0$ and $h = 0$. Explicit reference to these three examples is given in [18]. We point out a general scaling property of the Landau phase portraits. Because the profiles are obtained as specific sections of the phase portrait orbits, it is to be expected that the entire set of phase portraits has a scaling property. That is, portraits that correspond to different values of t and/or h and boundary conditions for different values of L could be made identical through appropriate rescaling of parameters. That this is indeed the case can be corroborated by examination of equations (4) and (2), as they can be rewritten as

$$\frac{\mathrm{d}\,(m/M)}{\mathrm{d}\,(z/\xi)} = \left[\left(\frac{m}{M}\right)^4 + \frac{at}{bM^2}\left(\frac{m}{M}\right)^2 - \frac{h}{bM^3}\frac{m}{M} + 1\right]^{1/2} \tag{12}$$

where $\xi \equiv \sqrt{A/2b}M^{-1}$, $M \equiv (C_L/b)^{1/4}$ and the quantities z/ξ, m/M, at/bM^2 and h/bM^3 are dimensionless. According to equation (12) the phase portrait in the scaled variables $\mathrm{d}\mu/\mathrm{d}x$ and μ, $\mu \equiv m/M$ and $x = z/\xi$ remains invariant. When $h = 0$ one has $M \propto (at/b)^{1/2}$, and when $t = 0$, $M \propto (h/b)^{1/3}$.

Acknowledgments

This work was supported partially by CONACyT grant 34572-E and by DGAPA-UNAM grant IN110100.

References

[1] Binder K 1983 *Phase Transitions and Critical Phenomena* vol 8 ed C Domb and J L Lebowitz (New York: Academic) p 1
[2] See, for example, 2001 Special issue on physical chemistry in confining geometries *Phys. Chem. Chem. Phys.* **3** 1155
[3] Thomson W T (Lord Kelvin) 1871 *Phil. Mag.* **42** 448
[4] Evans R 1990 *J. Phys.: Condens. Matter* **2** 8989 and references therein
[5] Binder K 1997 *Rep. Prog. Phys.* **60** 487 and references therein
[6] Sullivan D E and Telo da Gama M M 1986 *Fluid Interfacial Phenomena* ed C A Croxton (New York: Wiley) p 45
[7] Dietrich S 1988 *Phase Transitions and Critical Phenomena* vol 11 ed C Domb and J L Lebowitz (London: Academic)
[8] Nakanishi H and Fisher M E 1982 *Phys. Rev. Lett.* **49** 1565
[9] Landau D P, Ferrenberg A M and Binder K 2000 *Braz. J. Phys.* **30** 748 and references therein
[10] Lubensky T C and Rubin M H 1975 *Phys. Rev.* B **12** 3885
[11] Nakanishi H and Fisher M E 1983 *J. Chem. Phys.* **78** 3279
[12] Brochard-Wyart F and de Gennes P G 1983 *C.R. Acad. Sci., Paris II* **297** 223
[13] Parry A O and Evans R 1990 *Phys. Rev. Lett.* **64** 439
Parry A O and Evans R 1991 **66** 2175
Parry A O and Evans R 1992 *Physica* A **181** 250
[14] Swift M R, Owczarek A L and Indekeu J O 1991 *Europhys. Lett.* **14** 475
Swift M R, Owczarek A L and Indekeu J O 1991 *Phys. Rev. Lett.* **66** 2174
[15] Binder K, Landau D P and Ferrenberg A M 1995 *Phys. Rev. Lett.* **74** 298
[16] Rogiers J and Indekeu J O 1993 *Europhys. Lett.* **24** 21
[17] Carlon E and Drzewinski A 1997 *Phys. Rev. Lett.* **79** 1591
[18] Robledo A and Quintana J 1998 *Physica* A **257** 197
[19] Quintana J and Robledo A 1998 *Physica* A **248** 28
[20] See, for example, Priestley E B, Wojtowicz P J and Sheng P 1974 *Introduction to Liquid Crystals* (New York: Plenum)
[21] See, for example, Jacques J, Collet A and Wilden S H 1981 *Enantiomers, Racemates and Resolutions* (New York: Wiley)
[22] See, for example, Scott R L and van Konynenburg P H 1970 *Discuss. Faraday Soc.* **49** 81
van Konynenburg P H and Scott R L 1980 *Phil. Trans. R. Soc.* A **298** 495
[23] Quintana J and Robledo A 2001 *Physica* A **295** 333
[24] Wheeler J C and Widom B 1968 *J. Am. Chem. Soc.* **90** 3064
[25] Widom B 1984 *J. Phys. Chem.* **88** 6508
Widom B 1986 *J. Chem. Phys.* **84** 6943
[26] Robledo A 1987 *Phys. Rev.* A 36 4067
[27] Varea C and Robledo A 1981 *J. Chem. Phys.* **75** 5080